energies

MDPI

Article

Critical Benchmark Validation of the Core Physics Multigroup Cross-Section Library TPEX

Ying Chen [1], Haicheng Wu [1], Lili Wen [1,*], Yue Xiao [1], Jinchao Zhang [2], Qian Zhang [3], Xiaofei Wu [1] and Huanyu Zhang [1]

[1] China Nuclear Data Center, China Institute of Atomic Energy, Beijing 102413, China; chenying@ciae.ac.cn (Y.C.); wuhaicheng@ciae.ac.cn (H.W.); xiaoyue@ciae.ac.cn (Y.X.); wuxiaofei@ciae.ac.cn (X.W.); zhanghuanyu@ciae.ac.cn (H.Z.)
[2] College of Nuclear Science and Technology, Harbin Engineering University, Harbin 150001, China; 13935397912@hrbeu.edu.cn
[3] Department of Physics, Zhejiang University, Hangzhou 310030, China; zhangqian0515@zju.edu.cn
* Correspondence: wenlili@ciae.ac.cn

Abstract

Core physics multigroup cross-section libraries provide essential cross-section and burnup data for reactor neutron physics calculations, serving as a fundamental prerequisite for reactor physics analysis. The China Nuclear Data Center has developed the TPEX multigroup cross-section library for pressurized water reactors (PWRs) based on the Chinese Evaluated Nuclear Data Library CENDL-3.2. A systematic critical benchmark validation of the newly developed TPEX library has been performed. To verify its applicability and accuracy, the validation has been conducted against 131 critical benchmark experiments from the International Criticality Safety Benchmark Evaluation Project (ICSBEP 2006) and the WIMS-D library update project. The calculated effective multiplication factors (k_{eff}) are compared with the experimental values, results from equivalent multigroup libraries, and reference solutions from Monte Carlo code. The results indicate that the absolute average deviations between the calculated k_{eff} values using the TPEX library and the experimental measurements are 280 pcm for the uranium solution experiments, 410 pcm for the plutonium solution experiments, 10 pcm for the uranium metal lattice experiments, 20 pcm for the uranium dioxide lattice experiments, 22 pcm for the MOX fuel lattice experiments, and 150 pcm for the LCT001 uranium oxide assembly experiments. Accordingly, the TPEX library demonstrates excellent performance in reactivity predictions for PWRs.

Keywords: multigroup cross-section library; validation; CENDL-3.2; critical benchmark

Check for updates

Academic Editor: Fabio Moro

Received: 11 March 2026
Revised: 5 April 2026
Accepted: 16 April 2026
Published: 29 April 2026

Copyright: © 2026 by the authors. Licensee MDPI, Basel, Switzerland. This article is an open access article distributed under the terms and conditions of the Creative Commons Attribution (CC BY) license.

1. Introduction

Neutron physics calculations for nuclear reactors are the fundamental basis of reactor system design and safety analysis, with their computational accuracy exerting a direct impact on the assessment of reactor safety and economic performance. The core physics multigroup cross-section library provides cross-section and burnup data that are essential for neutron physics calculations in nuclear reactors, which act as a critical input for all numerical simulations. The accuracy of the multigroup cross-section data in the core physics library directly governs the precision of reactor physics calculations and subsequent design processes. Internationally representative lattice physics calculation codes (e.g., CASMO5 and HELIOS2) are typically accompanied by dedicated multigroup cross-section libraries developed from well-established evaluated nuclear data libraries, such as ENDF/B,

JEFF and JENDL. Confidence in these libraries is established through systematic critical benchmark validations. These validation efforts extensively cover a diverse range of experiments, such as thermal-spectrum solutions, fuel lattices and fuel assemblies, forming a comprehensive data validation framework that provides a solid foundation for the engineering application of multigroup cross-section libraries. For instance, the CASMO5 code has verified the accuracy of multigroup cross-section libraries developed based on the ENDF/B-VIII.0, ENDF/B-VIII.1. β2 and JENDL-5 libraries, respectively [1–3]. The DRAGON code has validated the DRALIB library constructed from the ENDF/B-VII.1 and JEFF3.1 libraries [4,5]. HELIOS2 has conducted verification of the multigroup cross-section library generated with the ENDF/B-VII.0 library [6]. PARAGON2 has confirmed the performance of the UFEML library derived from the ENDF/B-VII.1 library [7]. APOLLO2 has validated the APOLIB library developed using the JEFF-3.1.1 library [8]. In addition, the WIMS-D Library Update Project (WLUP) integrates a variety of evaluated nuclear data libraries and has systematically validated the accuracy of the WIMS-D library [9,10].

The Chinese Evaluated Nuclear Data Library (CENDL) has undergone decades of development, with the latest version, CENDL-3.2 [11], released in 2020. However, systematic critical validation efforts for the multigroup cross-section libraries developed on the basis of CENDL-3.2 remain relatively limited. The existing research is mostly limited to a small number of test cases, lacking category-based statistical analyses and error attribution studies conducted from the perspective of benchmark problem types. This research gap restricts understanding of its engineering applicability and impedes the popularization and application of CENDL-3.2 data in reactor design. To address this gap, the present study develops a 45-group multigroup cross-section library TPEX (hereinafter referred to as the TPEX library) based on TPAMS [12]—a core physics multigroup cross-section generation system developed by the China Nuclear Data Center. Subsequently, the deterministic calculation code ALPHA developed by Zhejiang University is employed to conduct systematic validation against 131 thermal-spectrum-critical benchmark experiments. These experiments are classified into three categories: uranium and plutonium solution experiments, designed to verify the fission spectrum data of key fissile nuclides; WLUP benchmark problems (including U-metal, UO_2 and MOX fuel lattice experiments), used to validate resonance-related data; and uranium oxide fuel assembly experiments, utilized to assess the accuracy of transport calculations for complex geometries. This study quantifies the accuracy and applicability of the TPEX library from three aspects—categorical statistical analysis of C/E biases, comparison with international multigroup libraries, and comparison with reference solutions from the Monte Carlo code JMCT [13]. It also analyzes the sources of biases and provides applicable validation conclusions for the engineering application of data based on CENDL-3.2.

This paper is organized as follows. Section 2 provides a detailed introduction to the TPEX library. Section 3 focuses on verification and validation, including a brief overview of the ALPHA code, calculation models and conditions, as well as the results and discussion related to the TPEX library. Finally, Section 4 summarizes the overall work and presents the corresponding conclusions.

2. Core Physics Multigroup Cross-Section Library TPEX

The TPAMS system includes an online input parameter library, a driver, a data processing program, and a test program. The procedure for generating a multigroup cross-section library based on TPAMS is illustrated in Figure 1 [12]. The TPEX library is generated by the TPAMS system and is developed based on CENDL-3.2. Decay data for the TPEX library are adopted from NuDat [14], and the effective fission yields are computed using the ENDF/B VII.1 library [15]. Thermal scattering law data utilized in the library are sourced from

ENDF/B VII.1, while the thermal scattering law for light water is evaluated by the CAB laboratory in Argentina. The TPEX library is a 45-neutron-energy-group library, consisting of 9 fast groups (20 MeV to 9.1188 keV), 16 resonance groups with shielded data (9.1188 keV to 1.8554 eV) and 20 thermal groups (below 1.8554 eV). The neutron energy group structure is defined as shown in Table 1. The TPEX library comprises a total of 649 nuclides. For non-moderator materials, the evaluated nuclide temperatures cover 293 K, 600 K, 900 K, 1200 K, 1500 K, 1800 K, 2100 K and 2500 K. For thermal scattering materials, the temperature grid is consistent with that adopted in the corresponding thermal scattering law files.

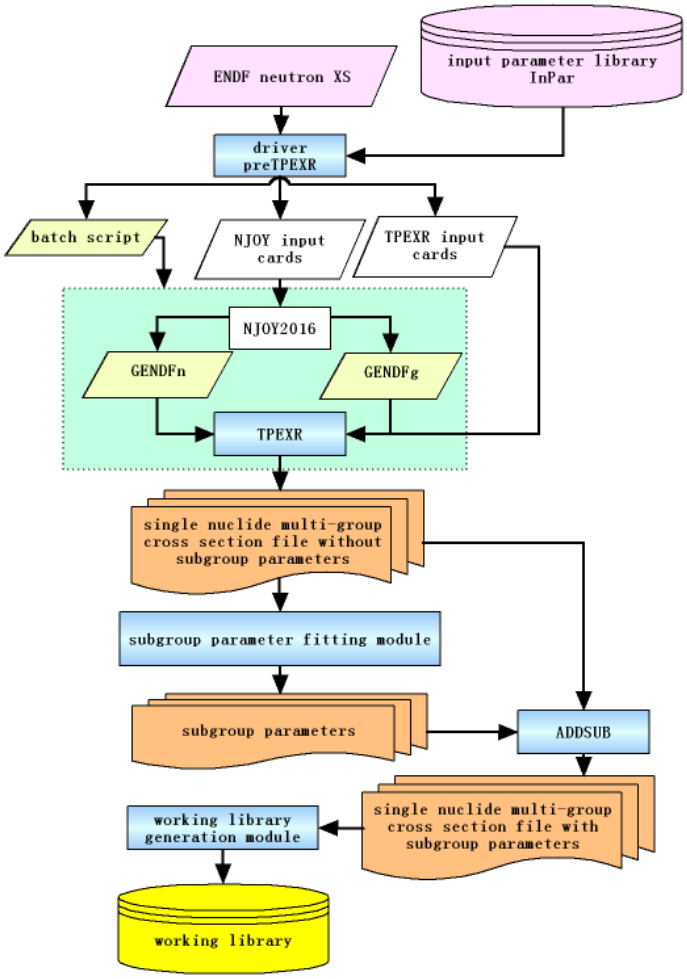


Figure 1. Procedure of generating multigroup cross-section library based on TPAMS. Source: Figure 1 from Reference [12].

There are several major data components that comprise TPEX library:

- Multigroup microscopic cross-section data for: σ_f, σ_a, σ_{tr}, σ_s, $\nu\sigma_f$ and P_0 scattering matrices;
- P_n scattering data (up to order 5 for nuclides where anisotropic scattering is important);
- Resonance data (shielding data tabulated at 16 and 32 background cross-sections and up to 8 temperatures spanning 293 K to 2500 K) and subgroup parameters;
- Goldstein–Lambda values and resonance upscatter data;
- (n, 2n) and (n, 3n) data;
- Neutron fission spectra;
- Fission yield and radioactive decay data and energy release per fission data;

Table 1. Neutron energy group structure.

Group	Energy (eV)	Group	Energy (eV)	Group	Energy (eV)
0	2.0000×10^{7}	16	1.2099×10^{1}	32	9.1000×10^{-1}
1	6.0653×10^{6}	17	8.3153×10^{0}	33	7.8208×10^{-1}
2	3.6788×10^{6}	18	7.3382×10^{0}	34	6.2506×10^{-1}
3	2.2313×10^{6}	19	6.4760×10^{0}	35	3.5767×10^{-1}
4	1.3534×10^{6}	20	5.7150×10^{0}	36	2.7052×10^{-1}
5	8.2085×10^{5}	21	5.0435×10^{0}	37	1.8443×10^{-1}
6	4.9787×10^{5}	22	4.4509×10^{0}	38	1.4572×10^{-1}
7	1.8316×10^{5}	23	3.9279×10^{0}	39	1.1157×10^{-1}
8	6.7379×10^{4}	24	2.3824×10^{0}	40	8.1968×10^{-2}
9	9.1188×10^{3}	25	1.8554×10^{0}	41	5.6922×10^{-2}
10	2.0347×10^{3}	26	1.4574×10^{0}	42	4.2755×10^{-2}
11	1.3007×10^{2}	27	1.2351×10^{0}	43	3.0613×10^{-2}
12	7.8893×10^{1}	28	1.1254×10^{0}	44	1.2396×10^{-2}
13	4.7851×10^{1}	29	1.0722×10^{0}	45	1.0000×10^{-4}
14	2.9023×10^{1}	30	1.0137×10^{0}		
15	1.3710×10^{1}	31	9.7100×10^{-1}		

3. Verification and Validation

Benchmarking refers to a research methodology that employs robust validation codes to perform calculations for well-characterized benchmark experiments, compares the computational predictions against the corresponding reference benchmark values, analyzes the sources of computational discrepancies, and thereby assesses the accuracy and reliability of a nuclear data library for the specific application scenarios represented by the benchmark experiments. Validation of the TPEX library not only provides data support for subsequent data adjustments within the library but also quantifies the numerical accuracy of the TPEX library corresponding to the specific application types represented by the benchmark experiments. This section describes the transport calculation code ALPHA utilized in the validation of the TPEX library, together with the computational results and numerical analyses of critical benchmark experiments.

3.1. ALPHA Code Description

ALPHA is a high-fidelity core neutron transport calculation code tailored for heterogeneous computing systems, developed at Zhejiang University. The flowchart associated with the ALPHA code is presented in Figure 2. The key numerical schemes and parallel implementation features of the ALPHA code are outlined as follows:

- Method of Characteristics (MoC) employed for core neutron transport calculations;
- Subgroup method adopted for resonance self-shielding computations;
- Performance-optimized 2D MoC computing kernel with native graphics processing unit (GPU) parallelization;
- Coarse- and fine-grained multi-node parallelization on heterogeneous systems implemented via a hybrid $MPI + CUDA$ programming model, coupled with communication-hiding optimization techniques.

3.2. Calculation Model and Condition

A total of 131 critical experiments selected from the ICSBEP 2006 and WLUP handbooks are adopted to validate the TPEX library, including 29 solution experiments, 95 lattice experiments and 7 assembly experiments. The calculation models and boundary condi-

tions corresponding to the three categories of experiments are elaborated separately in this section.

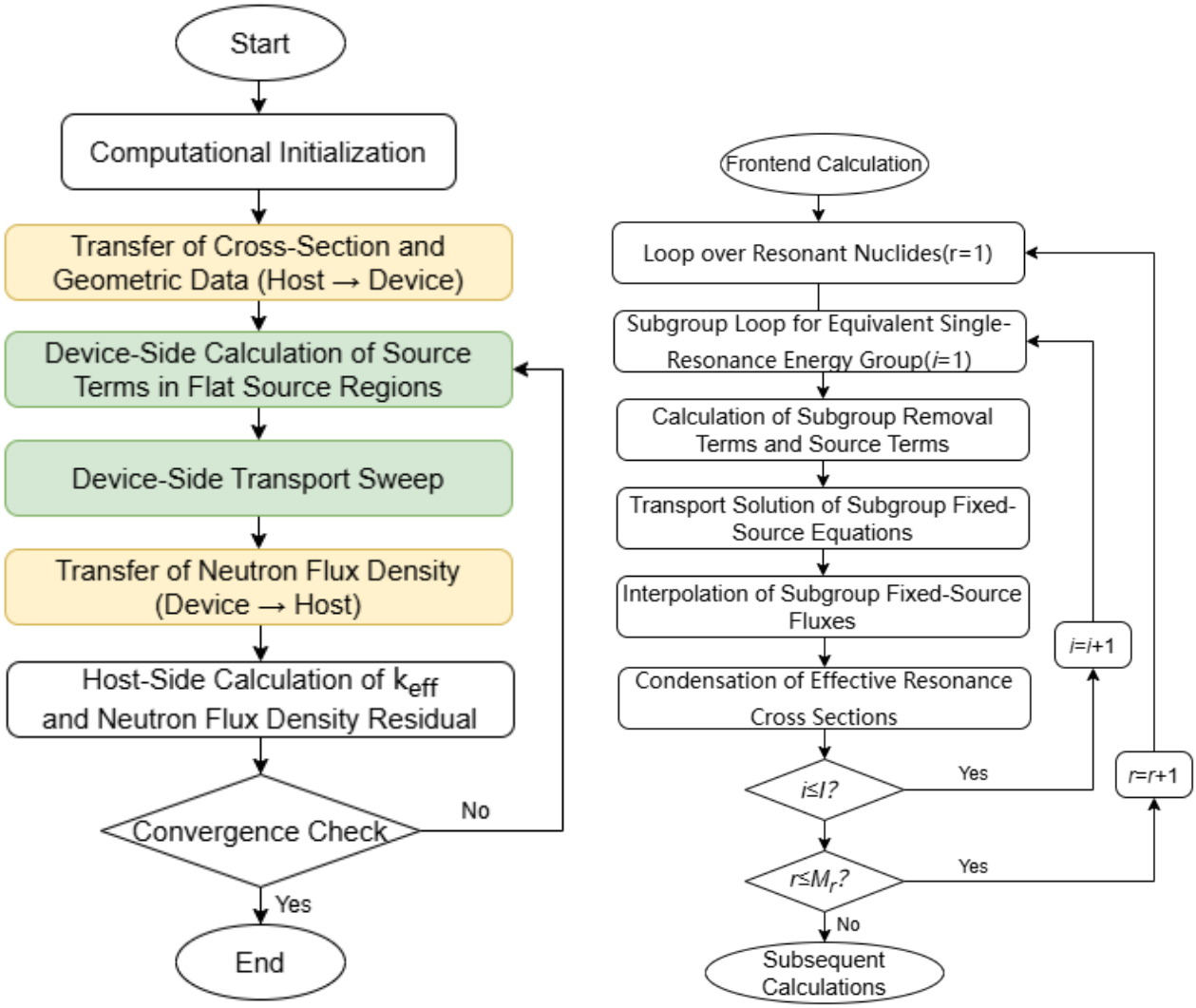


Figure 2. This is the flowchart for the ALPHA code: (**a**) GPU-accelerated parallel MoC Algorithm. (**b**) Circular logic of subgroup transport calculation.

3.2.1. Solution Experiments

A solution-filled spherical or cylindrical tank assembly can be approximated as a homogeneous model. Therefore, a two-dimensional single-cell model with reflective boundary conditions is adopted in the critical calculations for the solution experiments, and the geometric model established using the ALPHA code is presented in Figure 3. The experiments HEU-SOL-THERM-001, HEU-SOL-THERM-013, HEU-SOL-THERM-027, HEU-SOL-THERM-032, HEU-SOL-THERM-036, PU-SOL-THERM-011 and PU-SOL-THERM-021 are selected from ICSBEP 2006 for the validation. The material compositions and temperatures of the cell are taken from the relevant references [16].

Since components such as end plugs are not included in the criticality calculations of the ALPHA code, the JMCT [13] Monte Carlo code is utilized to perform calculations for both the detailed and simplified models of solution experiments to obtain k_{eff} and k_{∞}. A correction factor ξ is defined as the ratio of k_{eff} to k_{∞} to quantify the impact of these omitted components. The $k_{\infty,cal}$ output from the ALPHA code calculations is then corrected

using the correction factor ξ to derive the calculated value of the effective multiplication factor, $k_{eff,cal}$,

$$k_{eff,cal} = \xi k_{\infty,cal} \quad (1)$$

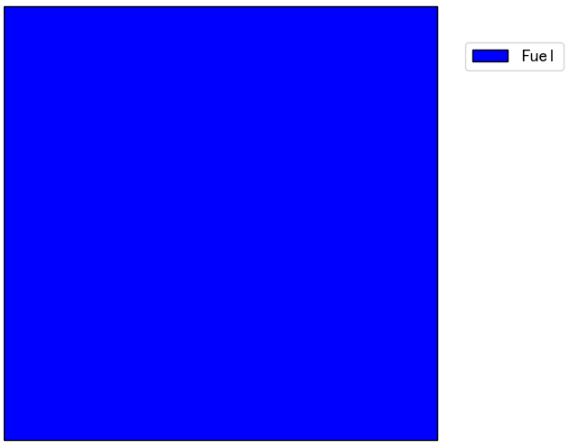


Figure 3. Geometry model for solution experiments.

3.2.2. WLUP Experiments

Several critical benchmark experiments are conducted under the WLUP to validate the WIMS-D library. A set of uranium metal, uranium oxide and MOX fuel experiments from the WLUP handbook are selected to validate the TPEX library. For modeling these experiments, two-dimensional single-cell models with reflective boundary conditions are employed. The geometric configurations comprise rectangular and hexagonal lattices, and axial buckling is used to account for neutron leakage in the axial direction. Of the 95 lattices investigated in this study, 3 are moderated by heavy water and the remainder by light water. Among the light water-moderated lattices, 53 use U-metal fuel, 15 use UO_2 fuel and 24 use MOX fuel. The ^{235}U enrichments vary from 0.928 to 4.43 wt%. V_{mod}/V_{fuel} varies from approximately 0.86 to 11.58. Fuel rod diameters from 1.03 cm to 6.868 cm are used; both stainless steel and aluminum clad are studied as well as both square and hexagonal lattice arrays. The data for all the cases are given in Table 2. The cell materials, material temperatures and axial buckling values are obtained from the WLUP handbook. The geometric models for all cases are established in strict accordance with the WLUP handbook. Given the large number of cases, schematic diagrams of four representative geometric models constructed using the ALPHA code are presented in Figure 4 herein.

Table 2. The data for all WLUP cases.

Case ID	Fuel Type	Number of Cases	Fuel Enrichment (wt%)	Lattice Pitch (cm)	Moderator	V_{mod}/V_{fuel}	q Value
UO_2 Cases							
AEEWJUNO	UO_2	1	3.003	1.87	H_2O	2.6	0.613
BAWcx10	UO_2	1	2.46	1.64	H_2O	1.84	0.579
BAY2b	UO_2	2	4.02	1.45–1.51	H_2O	0.96–1.14	0.465–0.488
WAPDcrx	UO_2	8	2.7–3.7	1.03–1.69	H_2O	1.05–4.98	0.505–0.635
BAPL	UO_2	3	1.31–4.43	1.11–1.81	H_2O	1.35–2.4	0.646–0.729

Table 2. *Cont.*

Case ID	Fuel Type	Number of Cases	Fuel Enrichment (wt%)	Lattice Pitch (cm)	Moderator	V_{mod}/V_{fuel}	q Value
U-Metal Cases							
AEREum	U-metal	4	0.928–1.142	4.267–4.75	H_2O	1.402–1.937	0.598–0.706
BNLum	U-metal	32	1.016–1.299	1.064–4.058	H_2O	1.0–4.0	0.54–0.803
HWum	U-metal	15	0.95–1.44	3.556–6.858	H_2O	0.86–2.92	0.536–0.748
TRX	U-metal	2	1.3	1.81–2.17	H_2O	2.35–4.02	0.621–0.711
MIT	U-metal	3	0.719	11.43–14.605	D_2O	20.76–34.61	
MOX Cases							
BNWpu	MOX	24	2.0–4.0	2.032–4.318	H_2O	1.486–11.58	0.534–0.87

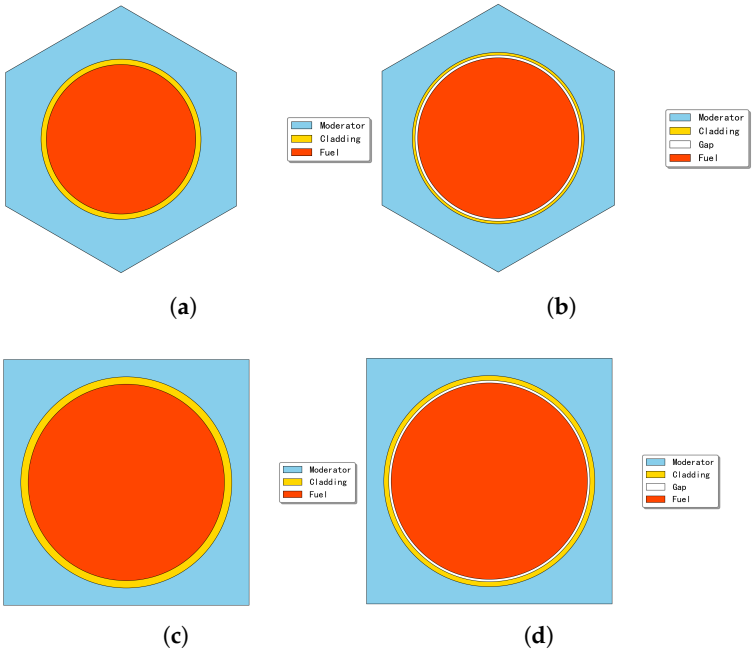


Figure 4. The geometric models established using the ALPHA code: (**a**) Typical three-region hexagonal model (fuel–clad–moderator). (**b**) Four-region hexagonal model (fuel–gap–clad–moderator). (**c**) Typical three-region rectangular model (fuel–clad–moderator). (**d**) Four-region rectangular model (fuel–gap–clad–moderator).

3.2.3. LCT001 Experiments

LEU-COMP-THERM-001 [16] in the ICSBEP 2006 handbook documents a series of critical experiments performed by the Pacific Northwest Laboratories (PNL), which employed clusters of aluminum clad $U(2.35)O_2$ fuel rods in a large water-filled tank (hereinafter abbreviated as LCT001). These experiments include rectangular square-pitched lattice clusters with pitches of 2.032 cm and no absorber plates, reflecting walls, dissolved poison, or gadolinium impurity.

2D assembly models are adopted in the ALPHA code for the simulation of this experimental series, with axial buckling employed to account for axial neutron leakage. Given the quarter symmetry of Cases 2–8, quarter-modeling is implemented for these cases, and the geometric models established with the ALPHA code are presented in Figure 5, where the left and upper boundaries are set as white reflective conditions and the right and lower boundaries as vacuum conditions.

Furthermore, since the measured axial buckling is not provided for the LCT001 experiments, it is necessary to derive this parameter via calculation. As indicated by Equation (2) for the reactor geometric buckling, the axial buckling can be calculated from the effective core height.

$$B_z^2 = \left(\frac{\pi}{z_{eff}}\right)^2, \tag{2}$$

The formula for the effective core height of a core with reflectors and end plugs is given in Equation (3), where the extrapolation distance $\lambda_{exp} = 0.7104\lambda_{tr} = 0.7104/\Sigma_{tr}$ and the diffusion length $L = \sqrt{\lambda_a \lambda_{tr}/3} = 1/\sqrt{3\Sigma_a \Sigma_{tr}}$. The transport cross-sections and absorption cross-sections are all calculated using the ALPHA code.

$$z_{eff} = z + 2\lambda_{exp} + \frac{L_{core}}{L_{plug}} z_{plug} + \frac{L_{core}}{L_{reflector}} z_{reflector} \tag{3}$$

The geometric and material information for the LCT001 experiments is presented in Table 3 and Table 4, respectively.

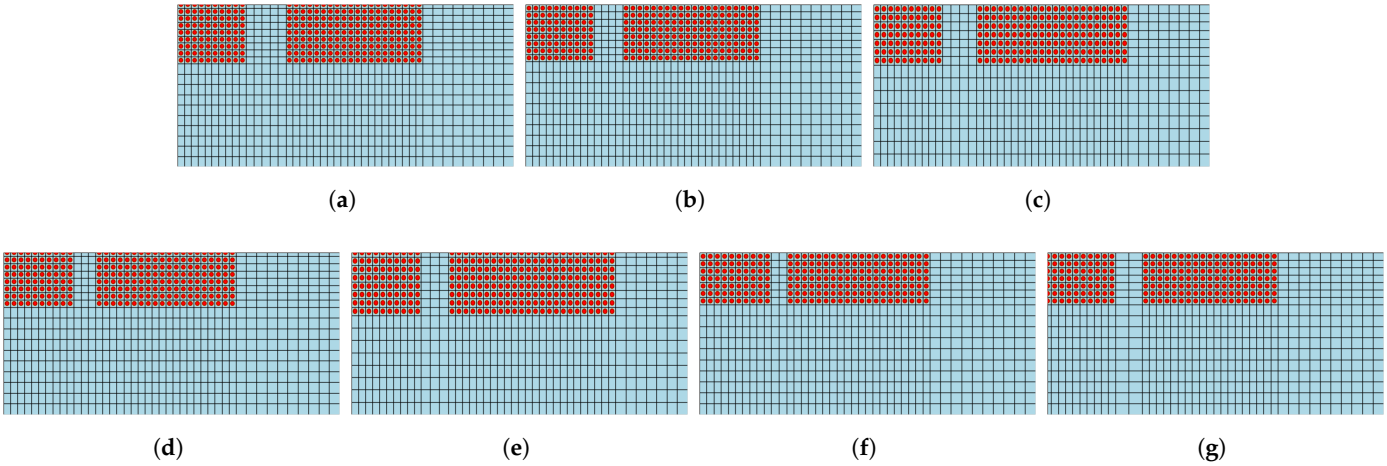


Figure 5. LCT001 geometric models established with the ALPHA code,where the red region represents the fuel and the blue region represents the moderator: (**a**) LCT001_02 case model. (**b**) LCT001_03 case model. (**c**) LCT001_04 case model. (**d**) LCT001_05 case model. (**e**) LCT001_06 case model. (**f**) LCT001_07 case model. (**g**) LCT001_08 case model.

Table 3. The geometric information for the LCT001 experiments.

Case ID	Number of Clusters	Cluster Dimensions (Number of Rods)	Separation Between Clusters (cm)	Effective Core Height (cm)	Axial Buckling
LCT001_02	3	20 × 17	11.92 ± 0.04	98.37844	1.019764×10^{-3}
LCT001_03	3	20 × 16	8.41 ± 0.05	98.380897	1.019714×10^{-3}
LCT001_04	3	20 × 16 (center) 22 × 16 (two outer)	10.05 ± 0.05	98.382035	1.019690×10^{-3}
LCT001_05	3	20 × 15	6.39 ± 0.05	98.378786	1.019757×10^{-3}
LCT001_06	3	20 × 15 (center) 24 × 15 (two outer)	8.01 ± 0.06	98.389029	1.019545×10^{-3}
LCT001_07	3	20 × 14	4.46 ± 0.10	98.37863	1.019761×10^{-3}
LCT001_08	3	19 × 16	7.57 ± 0.04	98.37553	1.019825×10^{-3}

Table 4. The material information for the LCT001 experiments.

Material	Isotope	wt.%	Atom Density (barn-cm)$^{-1}$
$U(2.35)O_2$ fuel	U-234	0.0137	2.8563×10^{-6}
	U-235	2.35	4.8785×10^{-4}
	U-236	0.0171	3.5348×10^{-6}
	U-238	97.62	2.0009×10^{-2}
	O	-	4.1202×10^{-2}
6061 Aluminum clad: 2.69 g/cm^3	Al	97.325	5.8433×10^{-2}
	Cr	0.2	6.2310×10^{-5}
	Cu	0.25	6.3731×10^{-5}
	Mg	1	6.6651×10^{-4}
	Mn	0.075	2.2115×10^{-5}
	Ti	0.075	2.5375×10^{-5}
	Zn	0.125	3.0967×10^{-5}
	Si	0.6	3.4607×10^{-4}
	Fe	0.35	1.0152×10^{-4}
Water	H	-	6.6706×10^{-2}
	O	-	3.3353×10^{-2}

3.3. Results and Discussion

This section presents the deviations between the experimental values and the calculated k_{eff} results obtained using the TPEX library and the ALPHA code, the H45 library (a 45-group library processed from ENDF/B-VI.8 [17]) with the ALPHA code, as well as the CENACE library derived from CENDL-3.2 with the JMCT Monte Carlo code. Furthermore, the accuracy and applicable scope of the TPEX library are discussed in detail on the basis of the numerical calculation results. In addition, a reduced chi-square value is calculated for all critical experiments to account for experimental uncertainties, as shown in the following equation.

$$\chi^2 = \frac{1}{N}\sum_{n=1}^{N}\left(\frac{k_{eff,n} - EXP_n}{uncertainty}\right)^2 \quad (4)$$

3.3.1. Solution Experiments

Tables 5 and 6 present the experimentally measured k_{eff} values and the corresponding calculated results from various libraries for the uranium solution-critical experiments and plutonium solution-critical experiments, respectively. The EALF values listed in the table denote the energy spectral index, which characterizes the energy characteristics of the relevant experiments. It serves as the benchmark reference for the experimental neutron spectrum indices in ICSBEP 2006 and represents a widely accepted international standard [16]. EALF represents the energy corresponding to the average neutron lethargy causing fission. The calculation formula is presented in Equation (5). The average neutron lethargy causing fission is defined for group calculations by the right-hand side of Equation (5).

$$EALF = \frac{E_0}{e^{\bar{u}}}, \bar{u} = \frac{\sum_m \sum_g (\bar{u_g} \times \Sigma_{f,g}^m \phi_g^m)}{\sum_m \sum_g (\Sigma_{f,g}^m \phi_g^m)} \quad (5)$$

where m is a physical zone inside the core; u_g is the midpoint of the g^{th} lethargy group, defined as lethargy of neutron with energy $\bar{E_g} = \sqrt{E_g E_{g-1}}$; $\Sigma_{f,g}$ is the group macroscopic fission cross-section; and ϕ_g is the neutron flux within lethargy group g. Lethargy u of a neutron with energy E is defined as $ln(E_0/E)$, where E_0 is defined as 10 MeV. A higher

EALF value indicates a harder energy spectrum for the selected experiment, and a smaller value indicates a softer energy spectrum for the experiment. The columns of $k_{eff,MC}$ and $k_{inf,MC}$ in the table correspond to the calculation results of the detailed model and the simplified model obtained with the JMCT code, respectively. Figure 6 shows the variation in C/E with EALF for the solution experiments.

Table 5. Calculation results for uranium solution experiments.

Case ID	EALF (eV)	EXP	Uncertainty	$k_{eff,mc}$	$k_{inf,mc}$	ξ	k_{inf}		k_{eff}	
							TPEX	H45	TPEX	H45
HST001_01	0.0814	1.0004	0.0060	0.9963	1.8263	0.5455	1.8380	1.8256	1.0027	0.9959
HST001_02	0.272	1.0021	0.0072	0.9941	1.8559	0.5356	1.8694	1.8550	1.0013	0.9936
HST001_03	0.0801	1.0003	0.0035	0.9999	1.8241	0.5482	1.8358	1.8234	1.0063	0.9995
HST001_04	0.292	1.0008	0.0053	0.9964	1.8546	0.5373	1.8683	1.8539	1.0038	0.9960
HST001_05	0.0431	1.0001	0.0049	0.9968	1.6259	0.6131	1.6374	1.6239	1.0039	0.9956
HST001_06	0.0446	1.0002	0.0046	1.0005	1.6508	0.6061	1.6624	1.6490	1.0076	0.9995
HST001_07	0.0773	1.0008	0.004	0.9958	1.8195	0.5473	1.8312	1.8188	1.0022	0.9954
HST001_08	0.0817	0.9998	0.0038	0.9962	1.8263	0.5454	1.8380	1.8256	1.0025	0.9957
HST001_09	0.292	1.0008	0.0054	0.9926	1.8546	0.5352	1.8683	1.8539	0.9999	0.9921
HST001_10	0.0462	0.9993	0.0054	0.9914	1.6706	0.5934	1.6822	1.6690	0.9983	0.9904
HST013_01	0.0327	1.0012	0.0026	0.9968	1.2138	0.8212	1.2253	1.2103	1.0062	0.9939
HST013_02	0.0341	1.0007	0.0036	0.9961	1.2087	0.8241	1.2191	1.2066	1.0047	0.9944
HST013_03	0.0355	1.0009	0.0036	0.9928	1.2013	0.8265	1.2108	1.2002	1.0007	0.9919
HST013_04	0.0362	1.0003	0.0036	0.9940	1.2005	0.8280	1.2101	1.2001	1.0019	0.9936
HST027_01	0.0742	1.0000	0.0046	0.9940	1.8057	0.5505	1.8169	1.8050	1.0002	0.9936
HST032_01	0.0313	1.0015	0.0026	0.9974	1.0718	0.9306	1.0826	1.0678	1.0075	0.9937
HST036_01	0.0559	0.9974	0.0045	0.9913	1.7419	0.5691	1.7530	1.7408	0.9977	0.9907
								Average	1.0028	0.9944
								χ^2	1.0373	2.6933

Table 6. Calculation results for plutonium solution experiments.

Case ID	EALF (eV)	EXP	Uncertainty	$k_{eff,mc}$	$k_{inf,mc}$	ξ	k_{inf}		k_{eff}	
							TPEX	H45	TPEX	H45
PST001_01	0.0885	1.0000	0.0050	0.9990	1.6918	0.5905	1.6850	1.6924	0.9950	0.9993
PST001_02	0.1120	1.0000	0.0050	1.0009	1.6925	0.5914	1.6831	1.6914	0.9953	1.0003
PST001_03	0.1370	1.0000	0.0050	1.0038	1.6915	0.5934	1.6798	1.6886	0.9969	1.0021
PST001_04	0.1540	1.0000	0.0050	0.9981	1.6876	0.5914	1.6750	1.6839	0.9906	0.9959
PST001_05	0.1620	1.0000	0.0050	1.0021	1.6872	0.5939	1.6738	1.6827	0.9941	0.9994
PST001_06	0.3670	1.0000	0.0050	1.0037	1.6604	0.6045	1.6426	1.6515	0.9929	0.9983
PST011_06	0.0517	1.0000	0.0052	0.9889	1.4524	0.6809	1.4570	1.4579	0.9920	0.9926
PST011_07	0.0527	1.0000	0.0052	0.9956	1.4619	0.6810	1.4666	1.4680	0.9987	0.9997
PST011_08	0.0526	1.0000	0.0052	0.9915	1.4570	0.6805	1.4615	1.4629	0.9946	0.9956
PST011_09	0.0537	1.0000	0.0052	0.9883	1.4618	0.6761	1.4661	1.4683	0.9912	0.9926
PST011_10	0.0550	1.0000	0.0052	0.9980	1.4663	0.6807	1.4704	1.4733	1.0008	1.0028
PST011_11	0.0584	1.0000	0.0052	0.9946	1.4830	0.6707	1.4866	1.4910	0.9970	0.9999
PST011_12	0.0536	1.0000	0.0052	0.9947	1.4680	0.6776	1.4723	1.4742	0.9976	0.9989
PST021_07	0.0610	1.0000	0.0032	1.0006	1.6030	0.6242	1.6066	1.6068	1.0028	1.0029
PST021_08	0.3240	1.0000	0.0065	0.9990	1.6451	0.6073	1.6461	1.6610	0.9996	1.0087
								Average	0.9959	0.9993
								χ^2	1.2086	0.6210

The numerical results indicate that the k_{eff} predictions using the TPEX library outperform those obtained with the H45 library for uranium solution-critical experiments. For

both libraries, the calculated k_{eff} values exhibit a decreasing trend as the neutron energy spectrum hardens within the EALF range of 0.02 eV to 0.06 eV, whereas an increasing trend in k_{eff} is observed as the spectrum hardens within the EALF range of 0.065 eV to 0.1 eV. In contrast, for plutonium solution-critical experiments, the k_{eff} values predicted by the TPEX library are generally lower than those predicted by the H45 library, with the H45 library demonstrating superior performance. To investigate the cause of the underprediction by the TPEX library in the PST experiments, the experiment PST001_04, which exhibits the lowest predicted k_{eff}, is selected as the research object. The effective fission cross-sections and effective absorption cross-sections of the material between the TPEX library and the H45 library are compared, as shown in Figure 7. The results indicate that the relative deviation in the effective fission cross-sections is small; however, the effective absorption cross-sections calculated by the TPEX library are significantly overestimated around 10 eV. This overestimation of absorption leads to the underprediction of k_{eff}. No consistent variation in k_{eff} with EALF is observed for the plutonium solution-critical experiments. Overall, the TPEX library exhibits superior predictive performance in solution-critical experiments, particularly for uranium solutions.

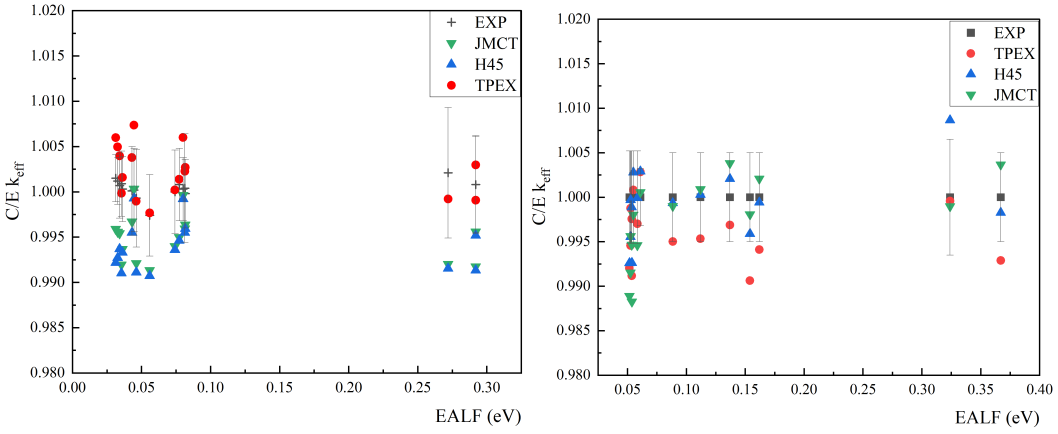


Figure 6. C/E k_{eff} results for solution experiments: (**a**) Dependence of C/E on EALF for uranium solution experiments. (**b**) Dependence of C/E on EALF for plutonium solution experiments.

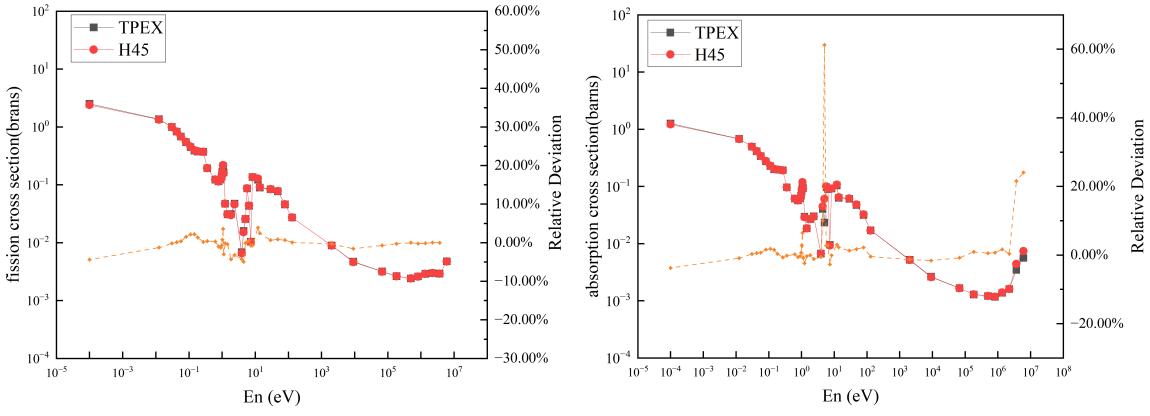


Figure 7. Effective cross-section results for PST001_04 experiment, where the orange line denotes the relative deviation between the H45 library and the TPEX library: (**a**) The effective fission cross-section results. (**b**) The effective absorption cross-section results.

3.3.2. WLUP Experiments

Due to the absence of three-dimensional experimental data for the WLUP experiments, the k_{eff} values predicted by the TPEX library are compared only with the experimental measurements and the results from the H45 library. Table 7 presents the experimentally measured k_{eff} values and the corresponding calculated results from various libraries for the uranium metal critical experiments. The q values listed in the table denote the number of fission neutrons that slow down below 2.6 eV. The q value characterizes the hardness of the spectrum and has a value of 1 for soft spectra in well-moderated low-absorbing lattices and is smaller for hard-spectrum lattices [9].

$$q = \frac{\sum_{g>2.5eV}(\phi_g \sum_{h<2.6eV} \Sigma_{s,g\to h})}{\sum_g \phi_g \nu_g \Sigma_{f,g}} \quad (6)$$

where ϕ_g is the cell spectrum from the region; $\Sigma_{s,g\to h}$ is the component of scattering matrix from group g to h; $\nu_g\Sigma_{f,g}$ is the macroscopic fission yield.

Table 7. Results for U-metal critical experiments.

Case ID	V_{mod}/V_{fuel} *	q Value	EXP	Uncertainty	k_{eff}	
					TPEX	H45
TRX-1	2.35	0.621	1.0000	0.003	0.9977	0.9940
TRX-2	4.02	0.711	1.0000	0.003	1.0037	0.9970
AEREuma3	1.402	0.639	1.0000	0.0033	0.9977	1.0023
AEREuma4	1.931	0.706	1.0000	0.0027	1.0010	1.0009
AEREumb1	1.407	0.598	1.0000	0.007	1.0026	1.0037
AEREumb2	1.937	0.66	1.0000	0.0025	0.9998	0.9972
BNLuma1	2	0.646	1.0000	0.0016	0.9979	0.9973
BNLuma2	3	0.712	1.0000	0.001	0.9969	0.9923
BNLuma3	4	0.764	1.0000	0.0012	1.0012	0.9950
BNLuma4	1.5	0.602	1.0000	0.001	0.9959	0.9991
BNLuma5	3	0.717	1.0000	0.001	0.9969	0.9920
BNLuma6	1	0.542	1.0000	0.0017	1.0005	1.0107
BNLuma7	4	0.797	1.0000	0.001	1.0008	0.9948
BNLumb1	1.5	0.599	1.0000	0.0049	0.9922	1.0011
BNLumb2	2	0.643	1.0000	0.0017	0.9999	0.9993
BNLumb3	3	0.709	1.0000	0.001	0.9982	0.9936
BNLumb4	4	0.761	1.0000	0.001	1.0001	0.9937
BNLumb5	1.5	0.599	1.0000	0.001	1.0001	1.0034
BNLumb6	2	0.645	1.0000	0.001	1.0007	0.9995
BNLumb7	3	0.714	1.0000	0.001	1.0007	0.9958
BNLumb8	4	0.771	1.0000	0.001	1.0005	0.9940
BNLumb9	1	0.54	1.0000	0.0017	0.9951	1.0103
BNLumb10	2	0.654	1.0000	0.001	0.9951	0.9946
BNLumb11	3	0.729	1.0000	0.001	1.0010	0.9967
BNLumb12	4	0.793	1.0000	0.0012	1.0033	0.9971
BNLumb13	1.334	0.592	1.0000	0.001	0.9959	1.0023
BNLumb14	2.334	0.691	1.0000	0.001	0.9995	0.9975
BNLumb15	2.834	0.731	1.0000	0.0029	0.9995	0.9958
BNLumb16	3.834	0.803	1.0000	0.0016	1.0027	0.9965
BNLumc1	4	0.733	1.0000	0.001	0.9977	0.9910
BNLumc2	1.5	0.584	1.0000	0.0021	0.9991	1.0020
BNLumd1	1.5	0.555	1.0000	0.001	1.0014	1.0021
BNLumd2	2	0.598	1.0000	0.001	0.9960	0.9926

Table 7. *Cont.*

Case ID	V_{mod}/V_{fuel} *	q Value	EXP	Uncertainty	k_{eff}	
					TPEX	H45
BNLumd3	3	0.661	1.0000	0.001	0.9997	0.9935
BNLumd4	3.018	0.662	1.0000	0.0023	1.0016	0.9955
BNLumd5	4	0.711	1.0000	0.001	1.0017	0.9944
BNLumd6	3	0.676	1.0000	0.001	1.0016	0.9960
BNLumd7	4	0.676	1.0000	0.001	1.0029	0.9957
HWuma1	1.2	0.61	1.0000	0.001	0.9966	1.0045
HWuma2	1.46	0.648	1.0000	0.001	0.9994	1.0037
HWuma3	1.72	0.682	1.0000	0.001	1.0024	1.0039
HWuma4	2.28	0.748	1.0000	0.001	1.0015	0.9995
HWumb1	1.37	0.606	1.0000	0.001	0.9984	1.0034
HWumb2	1.94	0.669	1.0000	0.001	1.0015	1.0021
HWumb3	2.15	0.689	1.0000	0.001	1.0084	1.0069
HWumb4	0.86	0.546	1.0000	0.001	0.9991	1.0113
HWumb5	1.33	0.631	1.0000	0.001	1.0005	1.0043
HWumb6	1.85	0.708	1.0000	0.001	1.0033	1.0024
HWumc1	1.21	0.536	1.0000	0.001	1.0026	1.0056
HWumc2	1.46	0.569	1.0000	0.001	1.0006	1.0009
HWumc3	1.73	0.6	1.0000	0.001	1.0031	1.0016
HWumc4	2.3	0.66	1.0000	0.001	1.0046	1.0005
HWumc5	2.92	0.719	1.0000	0.001	1.0058	0.9997
				Average	1.0001	0.9993
				St.dev. (pcm)	289	487
				χ^2	6.1472	19.201

* V_{mod}/V_{fuel}—the moderator-to-fuel volume ratio in the lattice, consistently defined in subsequent tables.

It can be seen from Table 7 that the k_{eff} values predicted by the TPEX library are superior to those by the H45 library, with a lower standard deviation as well. Figure 8 presents the calculated C/E k_{eff} results for uranium metal critical experiments.

According to the results in the figures, the k_{eff} values predicted by the H45 library exhibit an obvious negative correlation with the increase in V_{mod}/V_{fuel}, whereas no distinct regular variation is observed for the TPEX library. With the increase in the q value, i.e., the softening of the neutron energy spectrum, the k_{eff} values predicted by the H45 library show a decreasing trend. For the BNLum-series experiments, the k_{eff} values predicted by the TPEX library display a slight increasing trend with the rise in the q value, and this trend is more pronounced for the HWum-series experiments.

Table 8 summarizes the experimental k_{eff} measurements and the associated calculated outcomes from different libraries for the UO_2 experiments. Figure 9 presents the C/E ratios of k_{eff} for the UO_2 experiments. Table 8 demonstrates that the TPEX library yields a mean deviation of 20 pcm between the predicted k_{eff} values and experimental measurements, exhibiting superior predictive accuracy over the H45 library along with a lower standard deviation. As evidenced by Figure 9, the k_{eff} values predicted by the TPEX library show a slight increase with the rising q value. For the H45 library, the predicted k_{eff} increases with the softening of the neutron energy spectrum in the q range of 0.45–0.5, whereas a decreasing trend is observed with the further softening of the energy spectrum in the range of 0.5–0.65.

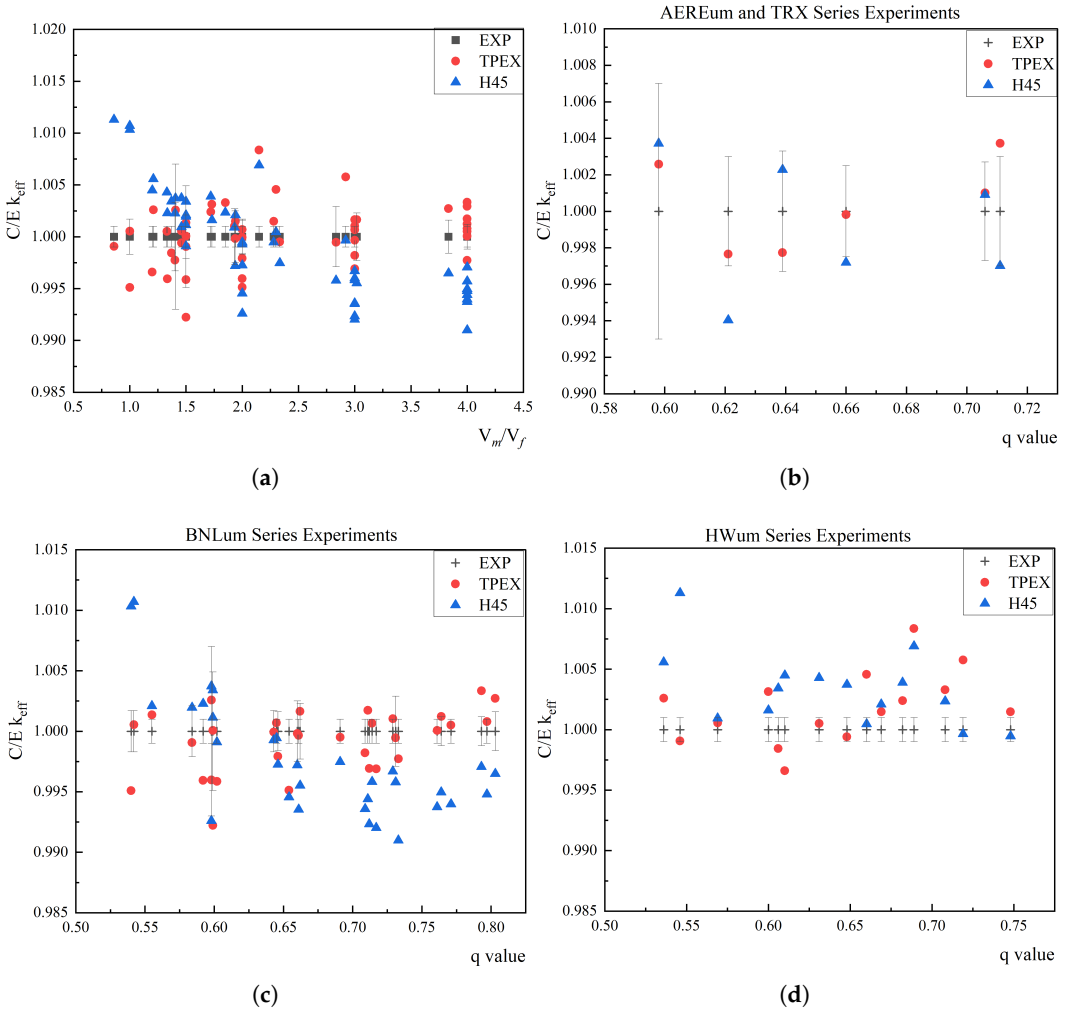


Figure 8. C/E k_{eff} results for uranium metal critical experiments: (**a**) C/E k_{eff} results as a function of V_{mod}/V_{fuel}. (**b**) Corresponding C/E k_{eff} variations with the q value for the AEREum-series experiments. (**c**) Corresponding C/E k_{eff} variations with the q value for the BNLum-series experiments. (**d**) Corresponding C/E k_{eff} variations with the q value for the HWum-series experiments.

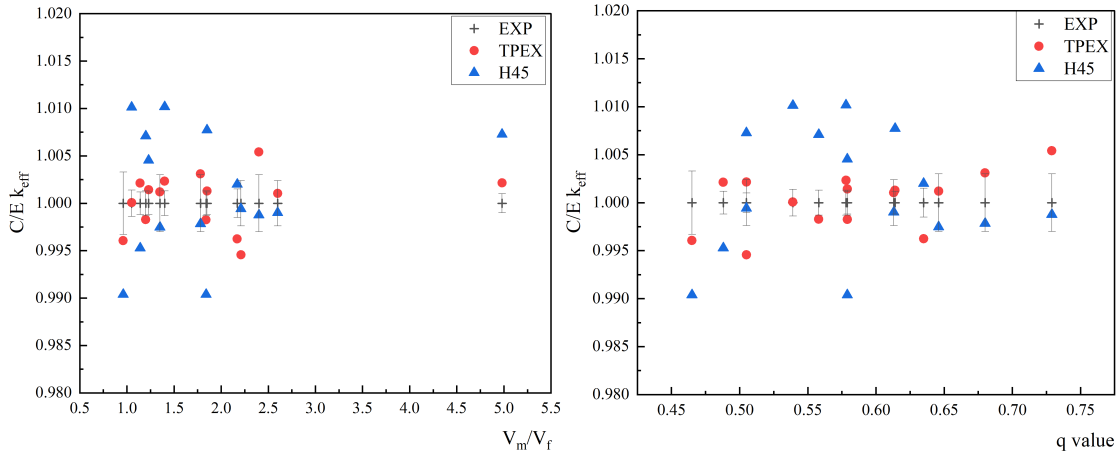
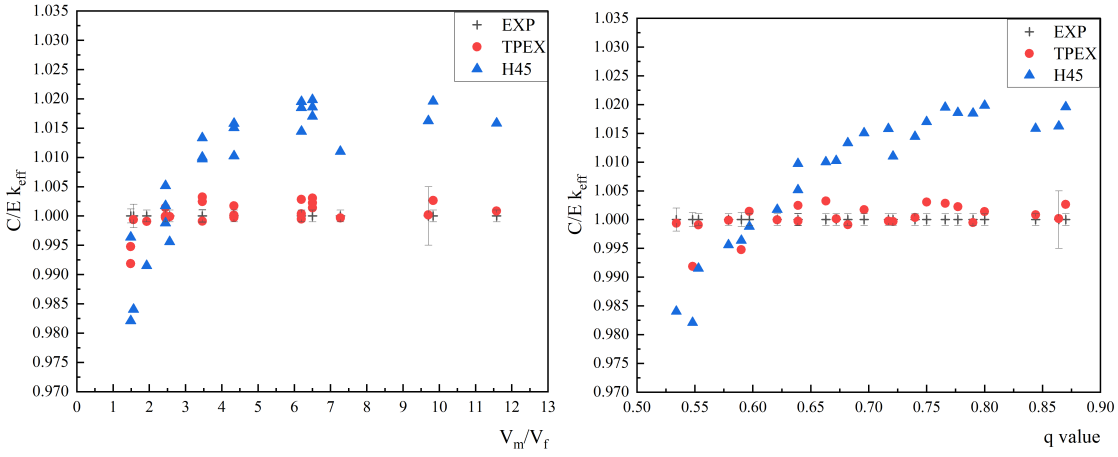


Figure 9. C/E k_{eff} results for UO_2 critical experiments: (**a**) C/E k_{eff} results as a function of V_{mod}/V_{fuel}. (**b**) Variation in C/E k_{eff} with the q value.

Table 8. Results for UO_2 critical experiments.

Case ID	V_{mod}/V_{fuel}	q Value	EXP	Uncertainty	k_{eff}	
					TPEX	H45
AEEWJUNO	2.6	0.613	1.0000	0.0024	1.0011	0.99901
BAWcx10	1.84	0.579	1.0000	0.0013	0.9983	0.99038
BAY2b1	0.96	0.465	1.0000	0.0033	0.9961	0.99038
BAY2b2	1.14	0.488	1.0000	0.0012	1.0021	0.99528
WAPDcrxa1	1.05	0.539	1.0000	0.0014	1.0001	1.01013
WAPDcrxa2	1.2	0.558	1.0000	0.0013	0.9983	1.0071
WAPDcrxa3	1.4	0.578	1.0000	0.0013	1.0023	1.01017
WAPDcrxa4	1.85	0.614	1.0000	0.0012	1.0013	1.00773
WAPDcrxa5	2.17	0.635	1.0000	0.0015	0.9963	1.00201
WAPDcrxb1	4.98	0.505	1.0000	0.001	1.0022	1.00727
WAPDcrxb2	1.23	0.579	1.0000	0.0012	1.0014	1.00453
WAPDcrxc	2.21	0.505	1.0000	0.0024	0.9946	0.99942
BAPL-1	1.35	0.646	1.0000	0.003	1.0012	0.9975
BAPL-2	1.78	0.68	1.0000	0.003	1.0031	0.9978
BAPL-3	2.4	0.729	1.0000	0.003	1.0054	0.9988
				Average	1.0002	1.0012
				St.dev. (pcm)	288	630
				χ^2	2.3092	22.2756

Table 9 lists the experimental k_{eff} values and the corresponding calculated results from various libraries for the MOX critical experiments. Figure 10 shows the C/E k_{eff} results of MOX fuel experiments. As can be observed from Table 9, the average deviation between the k_{eff} values predicted by the TPEX library and the experimental data is 22 pcm, which is considerably better than that of the H45 library, accompanied by a much lower standard deviation.



(**a**) (**b**)

Figure 10. C/E k_{eff} results for MOX critical experiments: (**a**) C/E k_{eff} results as a function of V_{mod}/V_{fuel}. (**b**) Variation in C/E k_{eff} with the q value.

According to Figure 10, the k_{eff} values calculated by the H45 library exhibit an obvious positive correlation with both the increasing q value and the rising V_{mod}/V_{fuel}. Considering the satisfactory performance of the H45 library in plutonium solution experiments, it is inferred that such discrepancies may arise from the inaccurate subgroup parameters of ^{239}Pu. The BNWpua8 experiment, which exhibits a significant overprediction of k_{eff}, is adopted as the study case. The energy-dependent effective absorption cross-sections in the

lattice, calculated using the TPEX library and the H45 library, are compared. As illustrated in Figure 11, the effective absorption cross-section computed with the H45 library is notably underestimated in the thermal energy region, leading to the overestimation of k_{eff}. In contrast, no evident systematic trend is observed in the k_{eff} values predicted by the TPEX library with the increase in either the q value or V_{mod}/V_{fuel}.

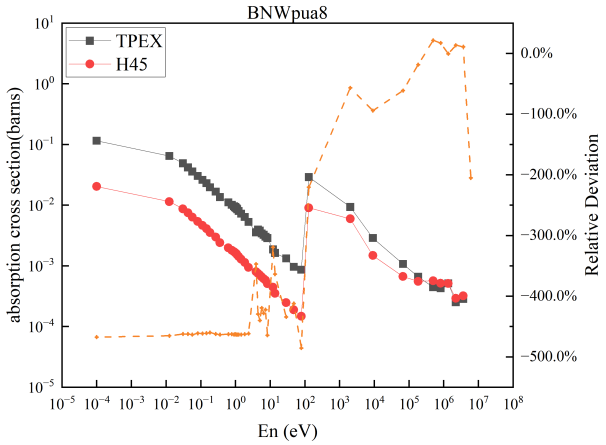


Figure 11. The effective absorption cross-section results for BNWpu8, where the orange line denotes the relative deviation between the H45 library and the TPEX library.

Table 9. Results for MOX critical experiments.

Case ID	V_{mod}/V_{fuel}	q Value	EXP	Uncertainty	k_{eff}	
					TPEX	H45
BNWpua1	1.486	0.548	1.0000	0.0012	0.9919	0.9821
BNWpua2	2.447	0.597	1.0000	0.001	1.0014	0.9988
BNWpua3	3.463	0.639	1.0000	0.0011	1.0025	1.0097
BNWpua4	4.335	0.672	1.0000	0.001	1.0001	1.0103
BNWpua5	6.196	0.74	1.0000	0.001	1.0004	1.0145
BNWpua6	6.501	0.75	1.0000	0.001	1.0031	1.0170
BNWpua7	9.696	0.864	1.0000	0.005	1.0002	1.0162
BNWpua8	9.831	0.87	1.0000	0.001	1.0027	1.0196
BNWpub1	2.447	0.621	1.0000	0.001	1.0000	1.0017
BNWpub2	3.463	0.663	1.0000	0.001	1.0032	1.0100
BNWpub3	4.335	0.696	1.0000	0.001	1.0017	1.0151
BNWpub4	6.196	0.766	1.0000	0.001	1.0028	1.0195
BNWpub5	6.501	0.777	1.0000	0.001	1.0022	1.0186
BNWpuc1	1.486	0.59	1.0000	0.0012	0.9948	0.9964
BNWpuc2	2.447	0.639	1.0000	0.001	0.9997	1.0052
BNWpuc3	3.463	0.682	1.0000	0.001	0.9991	1.0133
BNWpuc4	4.335	0.717	1.0000	0.001	0.9997	1.0158
BNWpuc5	6.196	0.79	1.0000	0.001	0.9995	1.0185
BNWpuc6	6.501	0.8	1.0000	0.001	1.0014	1.0199
BNWpud1	1.564	0.534	1.0000	0.002	0.9994	0.9841
BNWpud2	1.929	0.553	1.0000	0.001	0.9991	0.9915
BNWpud3	2.563	0.579	1.0000	0.001	0.9999	0.9956
BNWpud4	7.271	0.721	1.0000	0.001	0.9997	1.0110
BNWpud5	11.58	0.844	1.0000	0.001	1.0009	1.0158
				Average	1.00022	1.0083
				St.dev. (pcm)	249	1114
				χ^2	4.9952	170.106

Figure 12 presents the results for the MIT-series experiments moderated by heavy water. It can be observed from the figure that both the TPEX and H45 libraries yield accurate predictions of k_{eff}.

Collectively, the TPEX library demonstrates favorable predictive performance in the WLUP experiments and exhibits exceptional accuracy, particularly for MOX fuel experiments.

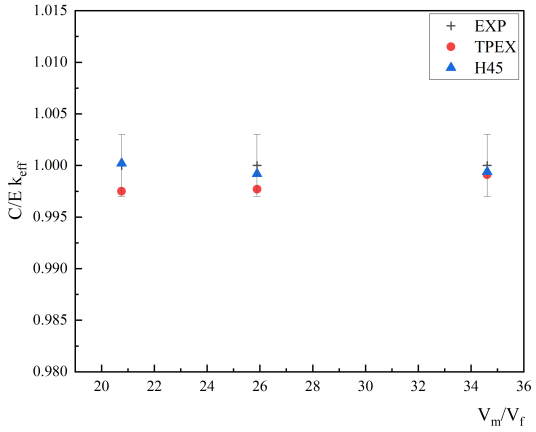


Figure 12. C/E k_{eff} results for MIT experiments.

3.3.3. LCT001 Experiments

Table 10 presents the experimental k_{eff} values and the corresponding calculated results from various libraries for the LCT001 experiment. Figure 13 illustrates the C/E k_{eff} values of LCT001. It can be observed from the above results that the average deviation between the k_{eff} values predicted by the TPEX library and the experimental data is 150 pcm, which is superior to that of the H45 library. Accordingly, the TPEX library also exhibits excellent performance in calculations involving complex geometries. Notably, the method used to calculate axial bulking assumes isotropic scattering, which tends to overestimate the effective height z_{eff}. This overestimation leads to an underestimation of bulking B_z^2, thereby reducing neutron leakage and causing an overestimation of k_{eff}. Consequently, the discrepancies between the k_{eff} values obtained from the TPEX library and the H45 library relative to the experimental data arise not only from multigroup cross-section data but also from errors introduced by the bulking approximation. As shown in the results presented in Table 10, the TPEX library overpredicts k_{eff} compared to the Monte Carlo results, which do not involve bulking treatment.

Table 10. Calculation results for LCT001 experiments.

Case ID	Separation *	EALF (eV)	EXP	Uncertainty	k_{eff}			C/E k_{eff}		
					TPEX	H45	JMCT	TPEX	H45	JMCT
LCT001_02	11.92	0.112	0.9998	0.0031	1.0019	0.9926	0.9977	1.0021	0.9928	0.9979
LCT001_03	8.41	0.111	0.9998	0.0031	1.0017	0.9925	0.9975	1.0019	0.9927	0.9977
LCT001_04	10.05	0.112	0.9998	0.0031	1.0021	0.9936	0.9981	1.0023	0.9938	0.9983
LCT001_05	6.39	0.11	0.9998	0.0031	0.9998	0.9903	0.9959	1.0000	0.9905	0.9961
LCT001_06	8.01	0.111	0.9998	0.0031	1.0019	0.9902	0.9978	1.0021	0.9904	0.9980
LCT001_07	4.46	0.109	0.9998	0.0031	0.9994	0.9904	0.9972	0.9996	0.9906	0.9974
LCT001_08	7.57	0.111	0.9998	0.0031	1.0025	0.9904	0.9961	1.0027	0.9906	0.9963
							Average	1.0015	0.9917	0.9974
							St.dev. (pcm)	112	132	80
							χ^2	0.3742	7.4215	0.7771

* Separation between clusters (cm).

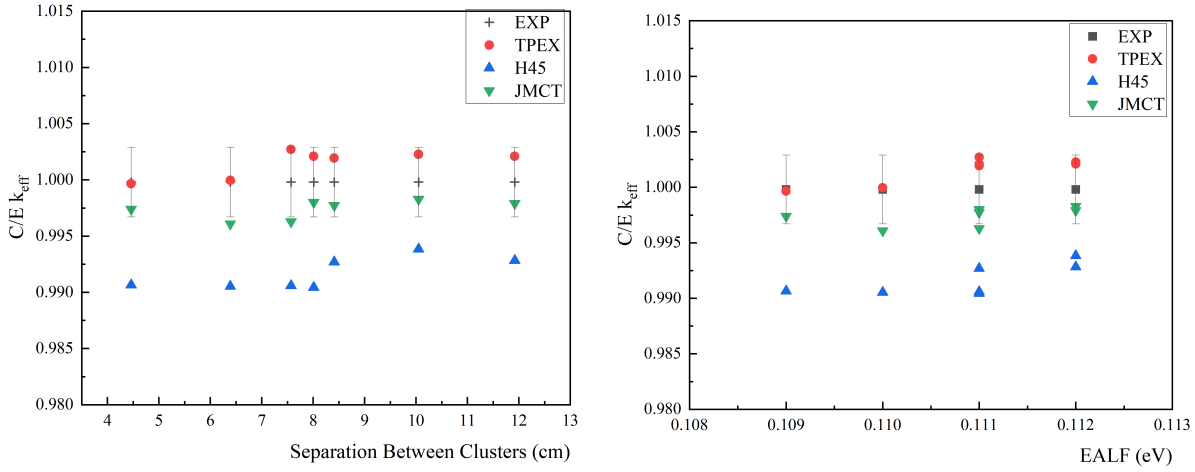


Figure 13. C/E k_{eff} results for LCT001 experiments: (**a**) C/E k_{eff} values of LCT001 as a function of the separation between clusters. (**b**) Variation in C/E k_{eff} with the EALF.

4. Conclusions

In this paper, a 45-group multigroup cross-section library designated as TPEX has been developed based on CENDL-3.2 and the core physics multigroup constant processing system TPAMS. Systematic validation is performed using the deterministic code ALPHA against 131 thermal-spectrum-critical experiments, covering uranium solution experiments, plutonium solution experiments, the WLUP series (including U-metal, UO_2 and MOX fuel lattice experiments), and thermal-spectrum uranium oxide fuel assembly experiments. The calculation accuracy and applicability of the TPEX library are evaluated by statistical analysis of C/E deviations, comparison with the H45 multigroup library derived from ENDF/B-VI.8, and verification against the reference solutions obtained with the Monte Carlo code JMCT. The main conclusions are drawn as follows:

Firstly, a dimension-reduction modeling approach for the three-dimensional experimental configurations has been implemented. For solution experiments, a model correction factor ξ is proposed. For three-dimensional experiments where the axial curvature is not explicitly provided, the axial curvature is derived from the effective height of the fuel assemblies. This treatment overcomes the limitation that lattice transport calculation codes cannot establish full three-dimensional models, thereby extending the validation scope of the multigroup cross-section library. Secondly, the numerical results indicate that the TPEX library exhibits excellent overall performance in thermal-spectrum-critical experiments. For solution-critical experiments with EALF in the range of 0.03–0.367 eV, the TPEX library yields smaller C/E deviations and lower standard deviations than the H45 library. The underestimation of k_{eff} observed in some calculations is mainly attributed to insufficient treatment of the resonance self-shielding for the radiative capture cross-section of ^{238}U. For the WLUP-series fuel lattice experiments with q values from 0.465 to 0.87, the TPEX library provides more accurate k_{eff} predictions with more stable trends and effectively mitigates the distinct systematic underestimation and strong sensitivity to energy spectrum and geometric parameters observed in the H45 library. For complex geometry assembly experiments such as LCT001, the TPEX library still maintains favorable predictive capability, demonstrating strong engineering applicability. In general, the TPEX library based on CENDL-3.2 exhibits high precision and reliability in thermal reactor physics computations and can provide significant validation support for engineering applications in reactor design and safety analysis.

Author Contributions: Conceptualization, H.W. and Y.C.; methodology, L.W.; software, J.Z. and Q.Z.; validation, Y.C., Y.X. and X.W.; formal analysis, H.W.; investigation, H.Z.; resources, X.W., Q.Z. and H.Z.; data curation, Y.C., L.W. and Y.X.; writing—original draft preparation, Y.C., H.W., Y.X. and J.Z.; writing—review and editing, L.W., Q.Z., X.W. and H.Z.; visualization, H.W., J.Z. and H.Z. All authors have read and agreed to the published version of the manuscript.

Funding: This work was financially supported by the Continuous-Support Basic Scientific Research Project and The APC was funded by China Institute of Atomic Energy.

Data Availability Statement: The original contributions presented in this study are included in the article. Further inquiries can be directed to the corresponding authors.

Conflicts of Interest: Authors Ying Chen, Haicheng Wu, Lili Wen, Yue Xiao, Xiaofei Wu and Huanyu Zhang were employed by China Institute of Atomic Energy. The remaining authors declare that the research was conducted in the absence of any commercial or financial relationships that could be construed as a potential conflict of interest. The authors declare that this study received funding from China Institute of Atomic Energy. The funder was not involved in the study design, collection, analysis, interpretation of data, the writing of this article or the decision to submit it for publication.

References

1. Margulis, M.; Blaise, P.; Ferrer, R.; Rhodes, J. Generation and initial validation of a new casmo5 endf/b-viii.0 nuclear data library. In *EPJ Web of Conferences*; EDP Sciences: Les Ulis, France, 2021; pp. 1–10.
2. Ferrer, R.; Wemple, C.; Hykes, J. Initial benchmarking of a new ENDF/B-VIII.1.β2-based CASMO5 neutron data library. In *International Conference on Physics of Reactors (PHYSOR 2024)*; American Nuclear Society: New York, NY, USA, 2024; pp. 778–789. [CrossRef]
3. Watanabe, T.; Suyama, K.; Tada, K.; Ferrer, R.; Hykes, J.; Wemple, C. Initial Verification and Validation of a New CASMO5 JENDL-5 Nuclear Data Library for Typical LWR Applications. *Nucl. Sci. Eng.* **2024**, *198*, 2230–2239. [CrossRef]
4. Jaï, O.; El Hajjaji, O.; Hébert, A.; Tajmouati, J.; El Bardouni, T.; Didi, A. Validation study of the reactor physics lattice transport code DRAGON5 based on DRAGLIB libraries by TRX and BAPL critical experiments of light water reactors for neutronic analysis of TRIGA MARK-II research reactor. *Mosc. Univ. Phys. Bull.* **2017**, *72*, 633–637. [CrossRef]
5. Al Zain, J.; El Hajjaji, O.; El Bardouni, T.; Lahdour, M. Validation of deterministic code DRAGON5 for the fuel depletion analysis of a PWR pin-cell benchmark. *Radiat. Phys. Chem.* **2021**, *186*, 109545. [CrossRef]
6. Wemple, C.; Simeonov, T. Advances in HELIOS2 nuclear data library. *Kerntechnik* **2017**, *82*, 445–447. [CrossRef]
7. Ouisloumen, M. Analyses of integral and mox critical experiments to qualify paragon2 predictions. In *EPJ Web of Conferences*; EDP Sciences: Les Ulis, France, 2021; Volume 247. [CrossRef]
8. Petrov, N.; Todorova, G.; Kolev, N.P. APOLLO2 and TRIPOLI4 solutions of the OECD VVER-1000 LEU and MOX assembly benchmark. *Ann. Nucl. Energy* **2013**, *55*, 93–107. [CrossRef]
9. Trkov, A.; Leszczynski, F.; Aldama, D. WIMS-D Library Update, Final Report of a Co-ordinated Research Project. In *IAEA*; Atomic Energy Agency: Vienna, Austria, 2006.
10. Malec, J.; Cabellos, O.; Kromar, M.; Trkov, A. Generation and validation of a new WIMS-D library based on ENDF/B-VIII.0. *Ann. Nucl. Energy* **2024**, *211*, 110989. [CrossRef]
11. Ge, Z.; Xu, R.; Wu, H.; Zhang, Y.; Chen, G.; Jin, Y.; Shu, N.; Chen, Y.; Tao, X.; Tian, Y.; et al. CENDL-3.2: The new version of chinese general purpose evaluated nuclear data library. *EPJ Web Conf.* **2020**, *239*, 09001. [CrossRef]
12. Wen, L.; Wu, H.; Chen, Y.; Chai, X.; Wu, X.; Tu, X.; Liu, Y. Development of multigroup cross section library generation system TPAMS. *Nucl. Eng. Technol.* **2024**, *56*, 2208–2219. [CrossRef]
13. Deng, L.; Li, G.; Zhang, B.; Li, R.; Shi, D.; Fu, Y.; Shangguan, D.; Hu, Z.; Zhang, L.; Peng, L. JMCT monte carlo code with capability of integrating nuclear system feedback. In *International Conference on Applied Mathematics, Modelling and Statistics Application (AMMSA 2018)*; Atlantis Press: Sanya, China, 2018. [CrossRef]
14. Sonzogni, A.A. NuDat 2.0: Nuclear Structure and Decay Data on the Internet. *AIP Conf. Proc.* **2005**, *769*, 574–577. [CrossRef]
15. Chadwick, M.B.; Herman, M.; Obložinský, P.; Dunn, M.E.; Danon, Y.; Kahler, A.C.; Smith, D.L.; Pritychenko, B.; Arbanas, G.; Arcilla, R.; et al. ENDF/B-VII.1 nuclear data for science and technology: Cross sections, covariances, fission product yields and decay data. *Nucl. Data Sheets* **2011**, *112*, 2887–2996. [CrossRef]

16. *International Handbook of Evaluated Criticality Safety Benchmark Experiments*; NEA/NSC/DOC(95)03; Nuclear Energy Agency: Paris, France; OECD: Paris, France, 2006.
17. Lemmel, H.D.; McLaughlin, P.K.; Pronyaev, V.G. *ENDF/B-VI Release 8 (Last Release of ENDF/B-VI)*; The U.S. Evaluated Nuclear Data Library for Neutron Reaction Data, IAEA-NDS-100, Rev.11; The U.S. Evaluated Nuclear Data Library: Upton, NY, USA, 2001.

Disclaimer/Publisher's Note: The statements, opinions and data contained in all publications are solely those of the individual author(s) and contributor(s) and not of MDPI and/or the editor(s). MDPI and/or the editor(s) disclaim responsibility for any injury to people or property resulting from any ideas, methods, instructions or products referred to in the content.